Pub. Astron. Soc. Pacific, Volume 86, August 1974

THE THEORY OF THE POLARIZATION OF CORONAL FORBIDDEN LINES*

LEWIS L. HOUSE
High Altitude Observatory, National Center for Atmospheric Research,† Boulder

Received 11 May 1974

A brief review, presented in simplified terms, is given for the theory of the origin of coronal emission-line polarization. A classical view of the scattering problem in terms of harmonic oscillators is first presented where the influence of the magnetic field is demonstrated. The Van Vleck depolarization phenomena is described in these terms. Next, a more precise physical picture of the emission-line polarization is established through a discussion of the Zeeman effect in scattering. Sample results are discussed for three-dimensional coronal emission-line models based upon the solution of the statistical equilibrium equations for magnetic sublevels of the Fe XIV ion. Finally, comments are directed toward the determination of magnetic fields based upon emission-line polarization observations where both modeling and deconvolution procedures are mentioned.

Key words: corona — polarization — magnetic fields — forbidden lines

I. Introduction

Encoded in the polarization of light scattered in the solar corona are clues to the structure of the magnetic fields in this tenuous, hot outer atmosphere of the sun. Magnetic fields are known to govern much of the shape and dynamics of the corona and it may be somewhat surprising that few systematic attempts have been made to establish the structure of the magnetic field by the most direct method, the measurement of linear polarization in the forbidden emission lines in the visible part of the coronal spectrum (cf. Charvin 1971; Eddy, Lee, and Emerson 1973). The shape of the corona shown in Plate I, taken during the 1966 eclipse, demonstrates clearly the complex structure that may be assumed by the million-degree plasma making up the solar corona. Many workers have been content to suppose that such a structure maps the distribution of magnetic fields, but for some problems more detailed knowledge of the orientation of the field is required. Researchers requiring this detailed knowledge have had to resort to extrapolation of magnetic fields from the surface of the sun into the corona, as described by Altschuler and Newkirk (1969). Since the extrapolation rests upon a fundamental theoretical assumption (not yet proven) that the coronal field is a potential field, it is very important to attempt to make systematic direct measurements of the magnetic field in the corona. The theory for the interpretation of such measurements is available (Charvin 1965; Hyder 1965; Hyder, Mauter and Shutt 1968; House 1972).

It is the purpose of this paper to describe in simple terms the origin of the polarization in the coronal emission lines, and to demonstrate how the polarization and the structure of the coronal magnetic field are related. We will first give a classical presentation of the concepts of radiation scattering in the presence of a magnetic field. Next, to show how one would construct a theoretical model to simulate the emission-line polarization of the corona, we will introduce some additional physical ideas using the Zeeman effect. And finally, we will discuss how the information that has been presented can be applied to establish the structure of coronal magnetic fields.

II. The Origin of Emission-Line Polarization: A Simplified View

It is the process of resonance fluorescence which gives rise to coronal emission-line polarization. Figure 1 depicts unpolarized radiation incident upon a scattering ion from the negative Z-direction. The ion is simulated by three

*Invited paper presented at the American Astronomical Society, Solar Physics Division Meeting, Honolulu, January 1974.

†The National Center for Atmospheric Research is sponsored by the National Science Foundation.

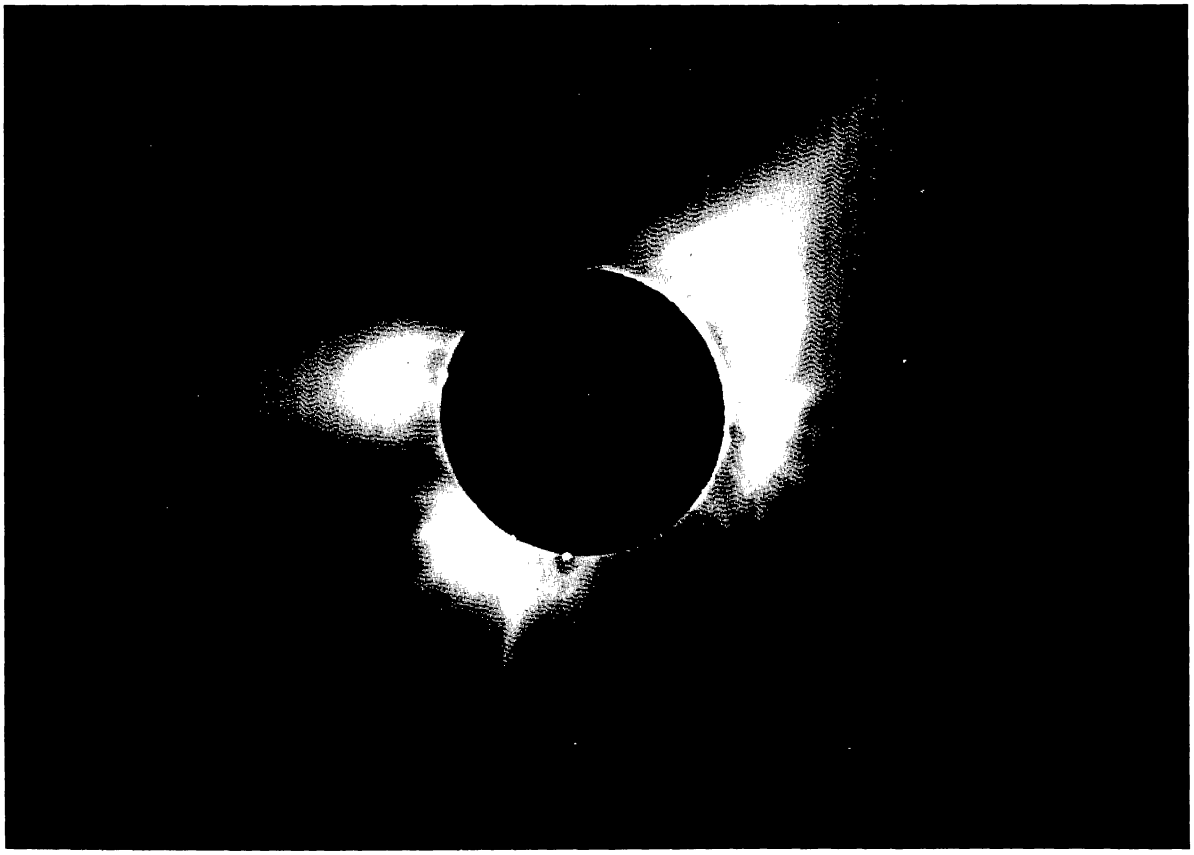

PLATE I

The solar corona observed by the High Altitude Observatory at the 1966 eclipse to Pulacayo, Bolivia. The structures as seen here in white light are assumed to map the distribution of magnetic fields.

orthogonal harmonic oscillators. The fact that the incident field is unpolarized is represented by equal intensities in two perpendicular states of linear polarization. The magnetic field, which lies along the x-axis, creates a direction of preferred orientation for the scattering ions; the ions precess about the magnetic field owing to the Larmor effect. We indicate the precession schematically by a coupling of the two oscillators that are perpendicular to the magnetic field. From the classical point of view, coupled oscillators will share any energy absorbed by a single oscillator. If the field is sufficiently strong, the oscillators are treated as completely coupled. The oscillator lying along the direction of the field, the x-oscillator, does not couple or share energy with either the y- or z-oscillators.

For the scattering in the forbidden lines of the solar corona it is appropriate, as we shall see later, to treat the y- and z-oscillators as completely coupled.

Now, recall that a harmonic oscillator absorbs and emits radiation according to the distribution shown in the insert on the lower right of Figure 1. The absorption- or emission-phase function relative to the direction of the axis of the oscillator, is a figure of revolution, a "doughnut" with no emission or absorption along its axis.

If we consider that the incident field has one unit of energy, one-half in each of the orthogonal components, the energy component absorbed by the oscillator lying along the y-axis will produce emission in both the y- and z-oscillators; since they are coupled, an amount proportional to one-quarter of a unit of the incident energy will be emitted from each of these oscillators. However, the energy absorbed by the oscillator lying along the magnetic field will be

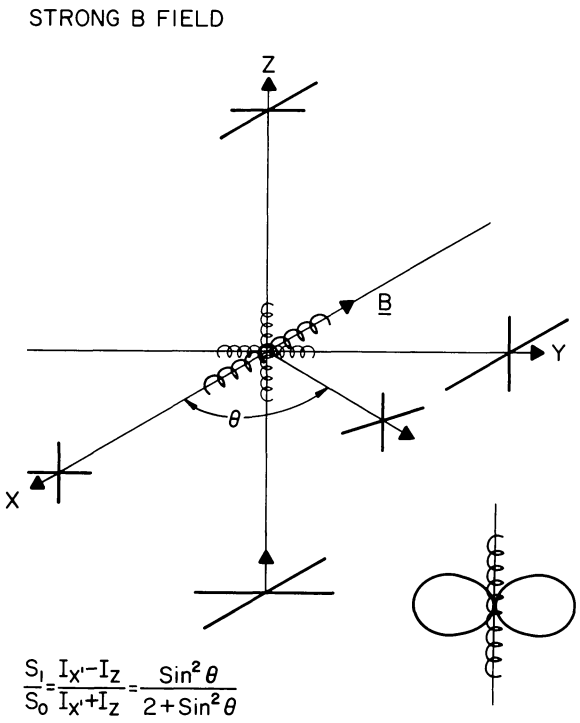

FIG. 1 — The scattering of radiation by an ion in the presence of a magnetic field. The detailed features of the diagram are discussed in the text.

reemitted only by that oscillator. Thus, if the observer looks along the y-axis, the energy polarized parallel to the z-axis and to the x-axis is in the ratio 2:1, respectively. Hence the degree of linear polarization, defined as the difference in intensity between two perpendicular directions divided by their sum, is 33%.

As the observer rotates toward the direction of the magnetic field a smaller fraction of the energy is emitted in the direction of the axis of the x-oscillator. Along the x-axis the radiation will be unpolarized because each of the oscillators emits an equal amount of energy in orthogonal polarization states, since they are coupled. Thus, from this model we see that the magnetic field produces between zero and 33% polarization depending upon the angle between the observer and the magnetic field. The polarization is axially symmetric about the field.

The amount of polarization in the $x-y$ plane is given by the simple expression included in the figure. All polarizations will be expressed in terms of the Stokes parameters. We need only consider the ratio of the Stokes parameter S_1, which describes the intensity of linearly polarized light, to the Stokes parameter S_0 describing the intensity of the radiation field. These are often known as the Q and I parameters, respectively. It is especially important to note that the maximum polarization will occur in a plane containing the magnetic field. That is, if we rotated a polaroid about the y-axis we would find the maximum polarization is parallel to the magnetic field.

If the magnetic field were not present, the coupling between the y- and z-oscillators would not occur. In this case an observer along the y-axis would see 100% linearly polarized light, polarized parallel to the x-axis. This would result from the fact that there would be no emission from the z-oscillator since it would absorb no radiation and no emission from the y-oscillator since we are looking along its axis. An observer looking along the z-axis would note unpolarized radiation because each oscillator viewed absorbs as well as emits in this direction.

If the magnetic field were present but parallel to the direction of the incident field, as might be the case for a radial field emerging from the surface of the sun, the results would be the same as if there were no field present. However, as we shall see later, the results for a radial field are significantly influenced by the fact that the magnetic field for various points along the line of sight through the corona goes through a range of angles.

From this discussion then, we see that there are significant differences introduced by the presence of a magnetic field.

Another interesting phenomenon resulting from the presence of the magnetic field is the so-called Van Vleck effect (Van Veleck 1925), which is depicted in Figure 2. Again we have a strong magnetic field and hence the complete coupling of two oscillators, but in this case the incident radiation propagation vector is not perpendicular to the magnetic field. The insert makes clear that one polarization component of the incident field lies in the $x-z$ plane while the other component is parallel to the x-axis. We simply look at the projections of the two components of the incident field to determine the relative amounts of radiation absorbed by each oscillator; these projections can be determined from the figure. When we consider the radia-

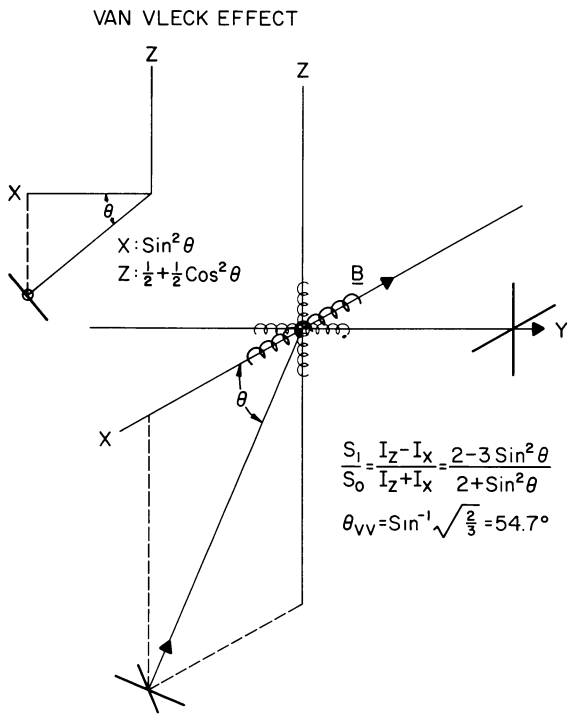

FIG. 2 — The Van Vleck effect which produces unpolarized radiation upon scattering in the presence of a magnetic field. The details of the effect are discussed in the text.

tion emitted by each oscillator, we find that the polarization, as observed perpendicular to the field, is given by the expression in the insert.

From this expression we note a very interesting property: the appropriate angle can produce zero polarization, that is, the scattered radiation field can be completely unpolarized. This, the Van Vleck effect, completely depolarizes scattered radiation when the incident field lies at an angle of 54°7 to the magnetic field. Furthermore, after the Van Veleck angle is passed the polarization is negative, which means that the plane of polarization is perpendicular to the magnetic field. It should be apparent that this effect can introduce difficulties into the interpretation of polarization data.

To summarize so far, we note that the polarization of the scattered radiation is very sensitive to the orientation of the magnetic field at the point of scattering. The magnetic field fixes the spatial orientation of the ions and locks their phase functions into a reference frame based upon the direction of the field. In the presence of a field, the radiation will be unpolarized along the field direction, as is also the case when the incident radiation meets the field at the Ven Vleck angle.

We shall now consider in more detail the nature of the coronal emission-line polarization problem as described by the Zeeman effect.

III. The Zeeman Effect in Scattering

In the presence of a magnetic field, the populations of magnetic sublevels of a given excited state of an ion determine the polarization properties of the emitted radiation. This is the more precise description of the origin of emission-line polarization. The manner in which the sublevels are populated is governed by the radiative and collisional coupling either to other sublevels of the same term or to magnetic substates belonging to the same or different configurations. The equations describing the statistical equilibrium of atomic states are well known (Mihalas 1970) except that now it has been necessary to generalize them to account for the fact that the equations become dependent upon geometry because of the presence of magnetic fields (Charvin 1965; House and Steinitz 1974*a*,*b*).

For background, it is necessary to establish some important properties for the coronal emission-line polarization problem. First we note that the corona is optically thin in the forbidden lines so that no radiative transfer or multiple scattering effects are present.

Next we need to understand the meaning of a "strong field" as it applies to the coronal problem. "Strong field" means that the Larmor frequency, ω_L, is greater than the inverse lifetime of the excited state, γ. Thus in a strong field an ion precesses many times between the absorption and reemission event. The critical field strength is given as

$$\frac{\omega_L}{\gamma} = \frac{eB_c g_{\rm eff}}{4\pi m_e c\gamma} = 1 \quad ,$$
$$B_c = 3.6 \times 10^{-7} A/g_{\rm eff} \quad , \qquad (1)$$

where e, m_e, and c have their usual meaning and where A is the Einstein transition probability and $g_{\rm eff}$ is the "effective" Lande g-factor. For forbidden lines, A is on the order of 100 $\sec^{-1}$, $g_{\rm eff} \sim 1$; thus the critical field is a few times 10^{-5} gauss and for essentially all coronal

regions we may justifiably use the strong field approximation.

Another ratio of interest is the ratio of the wavelength splitting due to the Zeeman effect compared to the Doppler width

$$\frac{\Delta\lambda_z}{\Delta\lambda_D} = \frac{eBg_{\text{eff}}}{4\pi m_e c} \Big/ \frac{\lambda}{c}\sqrt{(2KT/m)} \quad . \qquad (2)$$

For a 2-million-degree corona, this ratio is about 3×10^{-5} for a field of one gauss. Hence the splitting of a coronal forbidden line is extremely small. Furthermore, since to date all instruments that measure coronal emission-line polarization integrate over the entire profile, it can be shown, from the symmetry properties of the polarization averaged over line profiles, that there will be no circular polarization as a result of resonance fluorescence.

In Figure 3 we are reminded of the properties of the Zeeman pattern for the transition that we will use in our example, the line at 5303 Å belonging to the magnetic-dipole transition in the ground term of Fe XIV. The 5303 Å transition is a $^2P_{3/2}$ to a $^2P_{1/2}$ transition and it has the six Zeeman components indicated. The dashed lines refer to transitions where the magnetic quantum number m_J does not change, i.e., the π components, and the solid lines are those for a Δm_J of ± 1, the sigma components. It should be emphasized that each of the component transitions has its own relative strength factor as well as its own geometric phase function for absorption and emission. The relative-strength factors are easily established and are indicated in the figure, the $\Delta m_J = 0$ components above and the $\Delta m_J = \pm 1$ components below.

We consider two orthogonal linear polarization states, $\alpha = 0°$ and $\alpha = 90°$. The polarization vector $\alpha = 0°$ lies in the plane defined by the direction of the magnetic field and the observer. The $\Delta m_J = \pm 1$ transitions absorb isotropically for the polarization state $\alpha = 0°$, and according to a $\cos^2\theta$ function for the orthogonal state of polarization. The $\Delta m_J = 0$ components do not absorb or emit the polarization state $\alpha = 0°$, but absorb and emit in the polarization state $\alpha = 90°$ according to a $\sin^2\theta$ function. These geometric-polarization phase functions, each weighted by the relative strength of the appropriate transition, weighted also by the population of the sublevel, summed over all components in a Zeeman pattern, will then determine the polarization of the absorbed or emitted radiation.

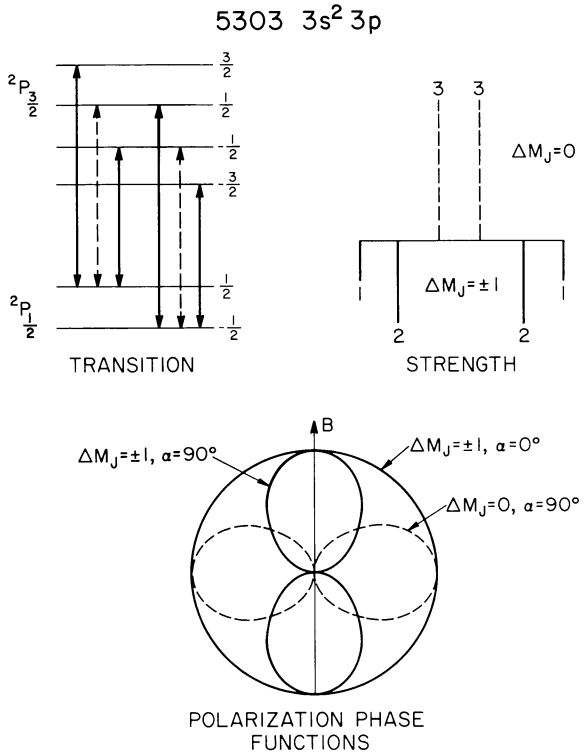

FIG. 3 — The Zeeman effect for the emission line λ5303 of Fe XIV. The six Zeeman transitions along with their strengths and polarization phase functions are illustrated.

With this information we can now discuss what goes into the solution of the equations of statistical equilibrium for the magnetic sublevels.

The energy level structure of Fe XIV is shown in Figure 4 where the ordinate for the left-hand side is approximately to scale, but the splitting into magnetic sublevels, on the right-hand side, is not drawn to scale. The configuration, the term, and the J value are indicated. The emission of the 5305 Å line arises from the $^2P_{3/2}$ term; we therefore need to determine the population of the magnetic sublevels belonging to this level. We must consider both radiative and collisional coupling, not only to the ground term of the configuration, but also to other configurations. In addition, we must consider how the coupling occurs, not only to other levels, but to other magnetic sublevels within those levels. It is possible that this coupling with excited configura-

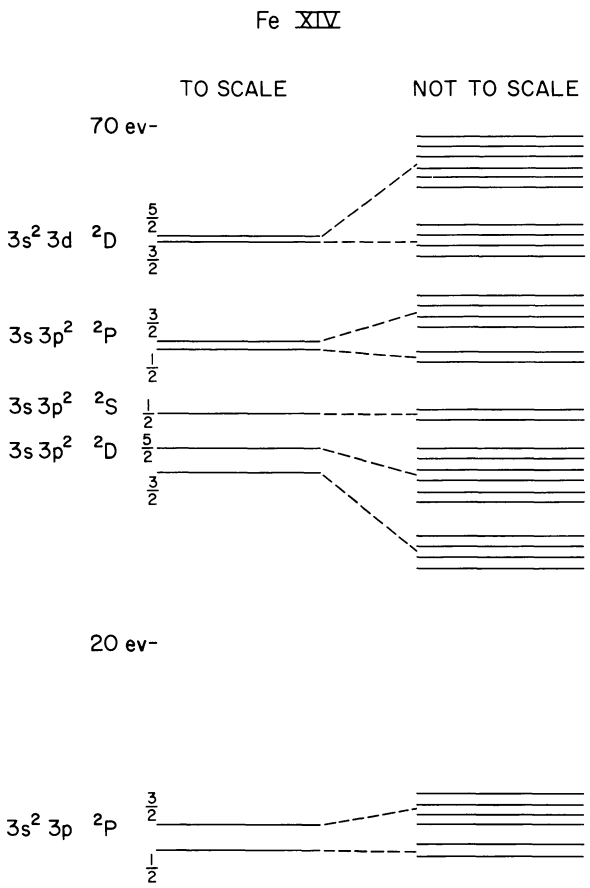

FIG. 4 — The energy level structure of the Fe XIV ion illustrating the splitting of the various levels into their magnetic sublevels.

tions may selectively populate or depopulate the magnetic sublevels that give rise to 5303 Å, and hence alter its polarization properties.

The physics that must go into setting up and solving the statistical equilibrium equations that will determine the population of each of the magnetic sublevels is summarized as follows. To establish the radiative rates one must integrate the appropriately combined phase functions for the Zeeman pattern of the transition over the incident unpolarized photospheric radiation field. This integration must account for limb-darkening. The calculation is carried out in a frame of reference of the local radius vector to the center of the sun and thus geometric transformations are involved. We neglect the radio frequency transitions that occur within the same level and we can neglect the ultraviolet absorption to excited configurations. The radiative rates are therefore easily established.

The collisional rates are much more difficult to determine. We must have the collisional rates to the level giving rise to 5303 Å as well as the rates to levels of the excited configurations. One difficulty that arises is that the total rates have been computed, but in the process of computing these total rates atomic physicists have averaged over the partitioning of the rates to the magnetic sublevels; hence little or no information is available at the present time as to how this partitioning should be made. Two extremes are that the collision strengths to magnetic sublevels are the same as for the radiative transition in the Zeeman pattern or that they are all equal. Information about collisional rates is desperately needed for this problem and work on it is now in progress.

The collisions that induce transitions between magnetic sublevels belonging to the same level are called depolarizing collisions. These collisions, occurring primarily by proton impact, effectively cause a reorientation of the ion between the absorption and emission event. This reorientation, if sufficiently randomized, depolarizes the emitted radiation. It should be apparent from classical Zeeman theory that the populations of the various magnetic sublevels are equivalent to the number of ions in the various possible quantized directions relative to the magnetic field. Thus transitions between sublevels are equivalent to changing the projection of the angular momentum states, or the orientation of the ions relative to the magnetic field.

Again, very little work has been done on computing depolarizing cross sections. Some simple semiclassical approximations borrowed from nuclear physics exist.

Finally note that we neglect, for the present, polarization induced by anisotropic beams of particles, by assuming that all collisions are produced by isotropic distributions.

Given procedures for determining the rates, then once the local electron temperature, density, and orientation of the magnetic field are established for a given volume of coronal plasma, the statistical equilibrium equations can be solved for the population of the magnetic sublevels. Again we emphasize that these equations are now angular dependent because the geometric

phase functions are oriented by the magnetic field.

After the populations of the magnetic sublevels have been computed, where in the case of the Fe XIV we use 34 magnetic sublevels, the populations of the excited state of 5303 Å may be put into equations to determine the Stokes parameters for the emission. Another geometric transformation must be performed to place these polarization results into a common frame of reference, the frame determined by the plane of the sky.

To compute a model of the emission-line corona, this procedure is carried through for many points along each line of sight for which information is desired. In addition one must also introduce the ionization equilibrium of the appropriate stage of ionization so that when the line-of-sight integration is performed, the correct weighting of the distribution of ions is accomplished. After the components of the Stokes vector are integrated along the line of sight, one finally has an emission-line polarization model for the solar corona. As described in the next section, such a model can be compared with observations to determine the appropriateness of the model parameters selected. Before we discuss the comparison of models with observations, let us next look at some of the results of sample solutions of statistical equilibrium equations. This will provide further insight into the physics of the formation of emission-line polarization.

Figure 5 shows plots of a parameter that measures the departure of the population of magnetic sublevels from their equilibrium populations. The parameter $\mathcal{L}$ can be defined by the following consideration. In thermodynamic equilibrium, each of the magnetic sublevels is equally populated and under this condition, for a given magnetic sublevel, we would assign a value of unity to the $\mathcal{L}$ parameter. Thus as $\mathcal{L}$ departs from unity it is a measure of the imbalance in the populations of the magnetic sublevels belonging to one term. The sum of the $\mathcal{L}$'s for a term is equal to the statistical weight.

For this plot we give the departure parameter $\mathcal{L}_{JM}$ versus height above the limb. We have assumed a radial magnetic field, the equatorial electron-density gradient as given by Newkirk, Dupree, and Schmahl (1970), and a constant

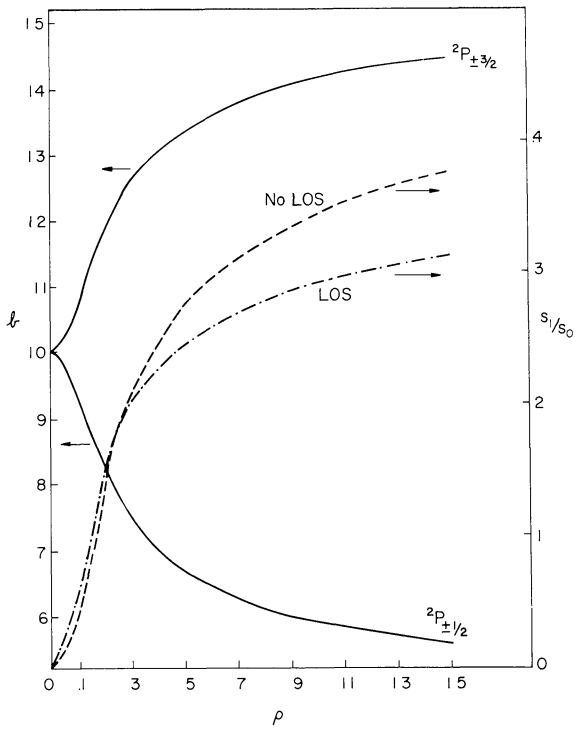

FIG. 5 — Plots of the departure coefficient for the magnetic sublevels giving rise to 5303 Å as a function of height. Also included in the plot is the resultant polarization as a function of height where the line-of-sight integration is included (LOS) and where the emission is only from the plane of the sky (No LOS). A radial magnetic field is assumed.

electron temperature. In addition we treat only the $^2P_{3/2}$ and $^2P_{1/2}$ levels. The plot shows how the increase in height, or equivalently the increase in anisotropy of the radiation field coupled with the decrease in density, causes the populations of the magnetic sublevels to depart from a balanced condition. The reason that the $m_J = \pm 3/2$ levels become over populated compared to the $m_J = \pm 1/2$ is that the $\pm 3/2$ levels are populated mainly by $\Delta m_J = \pm 1$ transitions which have phase functions, as you recall, that pick up radiation from the disk. On the other hand, the $m_J = \pm 1/2$ levels are mainly populated by $\Delta m_J = 0$ transitions whose phase functions $\sin^2\theta$ see less and less radiation from the disk as height is increased.

Included on the plot is the resulting degree of polarization from the 5303 Å radiation when we consider both the plane-of-the-sky emission (No LOS) and the effect of line-of-sight integration (LOS). The increasing departure of the

populations from equality produces an increased amount of polarization. This also occurs because the phase function and hence polarization properties of the emission from the different levels are weighted by the differing relative populations. Ultimately for 5303 Å the polarization at ∞ would be 43%.

The influence of the line-of-sight integrations is to decrease the polarization. This occurs for a radial magnetic field because field lines are presented to the observer at various orientations and we have seen that as one looks along the field, radiation is depolarized.

The next figure, Figure 6, again plots polarization versus height for the same model, i.e., for a radial field and the same temperature and density as for the preceding figure, but in this case we illustrate the influence of varying the number of levels in the Fe XIV model atom and of also varying the collisional coupling. The upper curve indicates what happens if we remove all collisions, both excitation and depolarization. This is the case of pure scattering. Clearly the polarization is much higher in pure scattering.

The middle curve represents the calculation

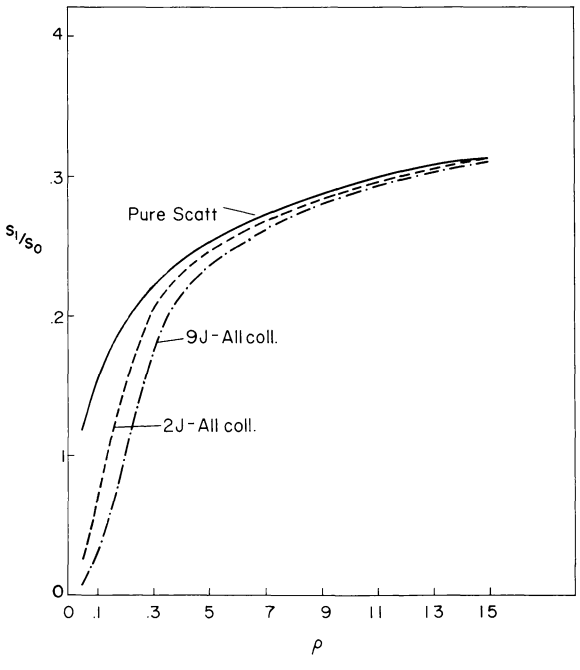

FIG. 6 — The degree of polarization as a function of height for the same model as in Figure 5, but with varying degrees of collisional coupling as well as differing numbers of energy levels included.

where only two J levels have been included, the $^2P_{3/2}$ and $^2P_{1/2}$ levels, while the bottom curve is for the case where we have included the excited configurations as shown previously on the energy level diagram for Fe XIV. In all, 34 magnetic sublevels were included. The effect of the excited levels is to decrease the imbalance between the populations of the $m_J = \pm 1/2$ and $\pm 3/2$ sublevels, which in turn produces a decrease in the polarization of the emitted radiation. The line-of-sight integration has been included in these calculations.

To conclude, we can now discuss how such a detailed understanding of the production of emission-line polarization will help us to eventually determine the orientation of magnetic fields in the corona, which of course is the ultimate goal.

IV. The Structure of Coronal Magnetic Fields from Emission-Line Polarization Measurements

There are two classical approaches in astrophysics for attempting to determine parameters of a stellar atmosphere, in this case the magnetic field structure. The first involves model building, where we assume the properties of the atmosphere and introduce what we know as the best possible physics. Theoretical predictions made from the model are then compared with observations, and if an agreement is reached we believe that the model may, in fact, simulate the real atmosphere. The result is not necessarily unique, of course. The other approach is to take the observational data and deconvolute it for the sought-after parameters. Both of these approaches can be considered in an attempt to determine the coronal magnetic field. Let us first look into the modeling approach.

A. *Modeling.* The solutions of the equilibrium equations and the resulting polarization models that have been described for examples result from a computer code that has much more general capabilities. We can summarize the major attributes of this code.

The code makes use of arbitrarily specified three-dimensional distributions of density, temperature, and magnetic field. It is most appropriate at the present time to take the three-dimensional electron-density data that result from the deconvolution of k-coronameter data

(Altschuler and Perry 1972). The best available model of coronal fields is that given by the potential field extension of photospheric fields into the corona (Altschuler and Newkirk 1969). Thus the program of the potential field calculation is coupled into the emission-lines polarization model calculation. There really exists no good model for the three-dimensional temperature distribution. The results are not terribly sensitive to temperature changes and often, as in the sample calculation of this paper, a uniform temperature corona will suffice.

With the coronal model specified, the computer program will treat any forbidden line for which collision rates and the Einstein coefficients can be provided.

The solution for the model involves all the geometric transformation eluded to, the integration of the incident field over the disk for each point in the corona, and the ionization equilibrium, resulting in the solution of the equilibrium equations. The populations thus determined are used to establish the Stokes parameters for the emission from each volume of coronal gas, and finally the integration is carried out for all lines of sight desired. The output of the program can give details on the population of energy levels, uv line intensities, etc. of the Fe XIV ion, but the main results are polarization and intensity maps.*

One such polarization map is shown in Figure 7. This computer model is for 5303 Å emission-line polarization at the time of the 1973 eclipse. The solid lines are the magnetic field lines based on a potential field, while the length of the short dashed lines is proportional to the degree of polarization. The lines are oriented to give the angle of maximum polarization with the center at the line of sight. A polarization vector having a length equal to the radius of the sun of this plot would be 100% polarized. The electron density is based upon the deconvolution of data provided by Mickey and Querfeld (1974).

This is a predicted model. If detailed, accurate observations were available to be compared to this model calculation, one could perhaps establish the validity of the assumption of a potential field distribution based upon the extrapolation of photospheric magnetic fields into the corona. For the most part one sees that the polarization vectors are mainly radial with some notable departures.

One interesting feature in the model calculation should be pointed out, and that is where we see the Van Vleck effect. In the southeast quadrant (lower right), polarization vectors are perpendicular to the direction of the field given by the potential field calculations. This is a region where the Van Vleck effect is present.

From the comparison of the model calculation with the potential field distribution upon which the model is based, it should be clear that if we are given only the polarization map, it is not an easy task to produce the distribution of magnetic fields.

B. *Deconvolution.* Final comments can be directed toward the possibility of determining the magnetic field orientation of the corona directly from the observational data rather than from a comparison with models.

First, we now realize that the Stokes parameter for the volume emission is buried inside integrals: the integral over the disk, for the incident radiation field, and the integral along the line of sight which samples a variety of orientations of magnetic fields. Next we note that the volume emission Stokes parameter is a function of the population of the magnetic sublevels that give rise to the forbidden line, and these populations are functions of the parameters of the corona, including the orientation of the magnetic field. Accordingly, we see that the angles for the field are rather deeply buried in the statistical equilibrium equations and therefore rather difficult to get at by direct deconvolution schemes.

There are indirect iterative schemes for deconvolution that are being pursued by Querfeld et al. (1974), but as yet no definitive results exist.

V. Conclusion

In this paper an attempt has been made, first in simplified terms, to describe some of the physics of the formation of emission-line polarization. The complete physics that must go into realistic calculations of coronal emission-line polarization has then been indicated, in somewhat more detail. Also, some of the difficulties

*This code resides in the High Altitude Observatory's Radiative Transfer Library and is available for public use.

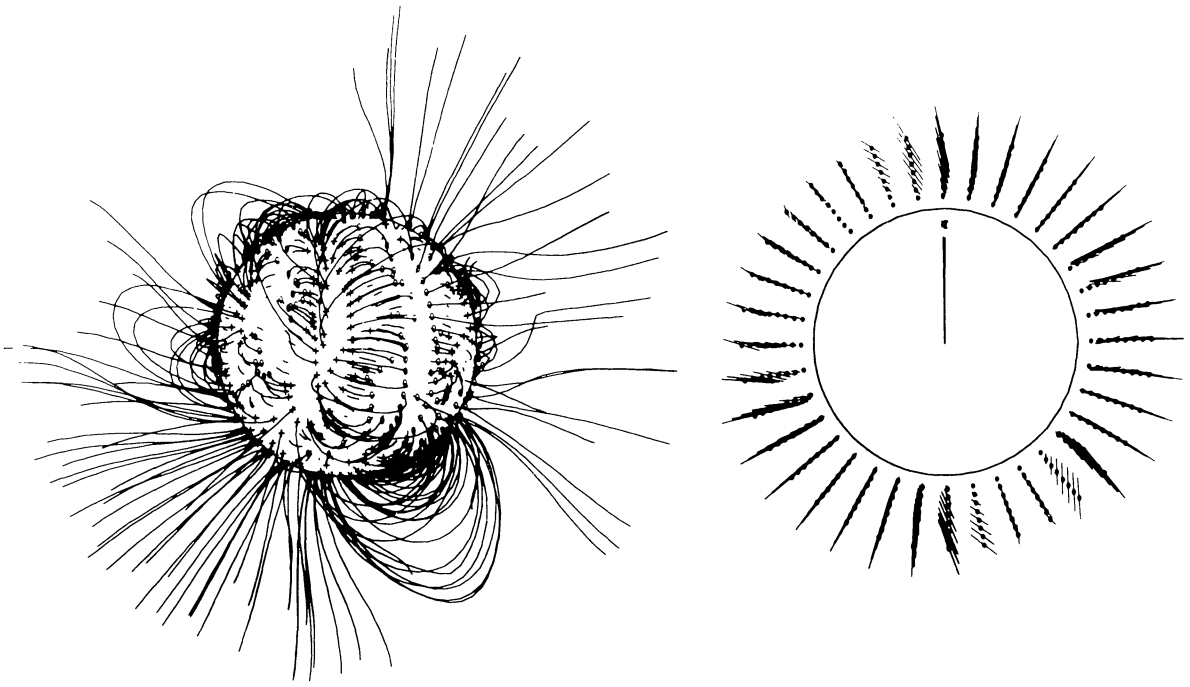

FIG. 7 — A potential field map of the magnetic field based upon photospheric data, and the accompanying theoretical polarization model of the 5303 Å emission line.

that are to be encountered in translating emission-line polarization observations into realistic maps of the coronal magnetic fields have been described. Clearly, it is a complicated problem to derive magnetic fields from the coronal emission-line polarization data, but the physics is available to guide our interpretations. It is perhaps because we do have a complete grasp of the physics of the problem that it appears complex. Many problems in astrophysics or solar physics seem simple only because much of the physics may be missing.

Through concentrated work on this problem, and with data available from both the University of Hawaii's 5303 Å polarimeter (Orrall 1971; Mickey 1973) and the High Altitude Observatory's coronal emission-line polarimeter (Querfeld 1974) that will measure the 10747 Å line of Fe XIII, it is hoped that one will be able to produce the sorely needed maps of the coronal magnetic fields in the near future.

REFERENCES

Altschuler, M. D., and Newkirk, G. A., Jr. 1969, *Solar Phys.* **9**, 131.

Altschuler, M. D., and Perry, R. M. 1972, *Solar Phys.* **23**, 410.

Charvin, P. 1965, *Ann. d'Ap.* **28**, 877.

—— 1971, in *Solar Magnetic Fields,* R. Howard, ed. (Dordrecht: D. Reidel Publishing Co.).

Eddy, J. A., Lee, R. H., and Emerson, J. P. 1973, *Solar Phys.* **30**, 351.

House, L. L. 1972, *Solar Phys.* **23**, 103.

House, L. L., and Steinitz, R. H. 1974*a*, *Ap. Letters* (in press).

—— 1974*b* submitted for publication.

Hyder, C. L. 1965, *Ap. J.* **141**, 1382.

Hyder, C. L., Mauter, H. A., and Shutt, R. C. 1968, *Ap. J.* **154**, 1039.

Mickey, D. L. 1973, *Ap. J. (Letters)* **181**, L19.

Mickey, D. L., and Querfeld, C. W. 1974, Paper presented at Solar Physics Division Meeting AAS, Honolulu, Hawaii, 1974.

Mihalas, D. 1970, *Stellar Atmospheres* (San Francisco: W. H. Freeman).

Newkirk, G. N., Dupree, R., and Schmahl, E. 1970, *Solar Phys.* **15**, 15.

Orrall, F. Q. 1971, in *Solar Magnetic Fields,* R. Howard, ed. (Dordrecht: D. Reidel Publishing Co.).

Querfeld, C. W. 1974, in *Planets, Stars and Nebulae Studied with Photopolarimetry,* T. Gehrels, ed. (Tucson: University of Arizona Press), p. 254.

Querfeld, C. W., Altschuler, M. D., Mickey, D. L., and House, L. L. 1974 (private communication).

Van Vleck, J. H. 1925, *Proc. Nat. Acad. Sci.* **11**, 612.